Theoretical treatment of electron-capture processes in ion-molecule collisions: $B^{3+}+H_2$ as a test case

M. C. Bacchus-Montabonel
Laboratoire de Spectrométrie Ionique et Moléculaire (UMR 5579), CNRS et Université Lyon I
43, Boulevard du 11 Novembre 1918, 69622 Villeurbanne Cedex, France
(Received 6 November 1998)

Ab initio potential-energy curves and coupling matrix elements of the molecular states involved in the collision of the $B^{3+}(^1S)$ multicharged ion on molecular hydrogen have been determined by means of configuration-interaction methods. The total and partial electron-capture cross sections have been evaluated in the frame of a semiclassical approach in the 10–170-keV laboratory energy range. Anisotropy and vibrational dependence have been examined, at both the molecular calculation and collision dynamics levels. [S1050-2947(99)06705-0]

PACS number(s): 34.70.+e

I. INTRODUCTION

Electron-capture processes of multiply charged ionic species in collision with neutral atoms or molecules are of considerable interest in controlled nuclear fusion research as well as in astrophysical plasmas. More and more attention is now beinng paid to charge-transfer reactions involving molecular targets, in particular molecular hydrogen, which may be possible dominant processes in astrophysical environments with low electron or atomic hydrogen abundances [1] and are also essential in tokamak fusion plasmas. From an experimental point of view, some data, mainly total cross sections, on collisions of carbon, oxygen, and, more recently, boron ions on a H_2 target are available, essentially at keV intermediate energies, as they have been stimulated by the need of precise information on impurity ion behavior. Nevertheless, while the theoretical treatment of ion-atom collisions has considerably progressed, relatively little detailed work has yet been done on ion-molecule reactions. The most complete studies are the $Be^{4+}+H_2$ and $C^{q+}+H_2$ treatments of Errea *et al.* [2–4], as well as the linear approach of the $N^{2+}+H_2$ collision [5].

We have thus undertaken a theoretical study of the $B^{3+}+H_2$ reaction involving an *ab initio* molecular calculation of the potential-energy surfaces and corresponding couplings followed by a semiclassical dynamics in the 10–170-keV laboratory energy range where experimental data are available [6–9]. Boron ions have indeed been the subject of increasing interest as impurity in controlled fusion reactions [10]; furthermore, the $B^{3+}+H_2$ system is a relatively simple closed-shell system for which only the $B^{2+}(1s^22s)$ and $B^{2+}(1s^22p)$ channels might be populated in single electron capture and could be considered as a benchmark for an approach on ion-molecule collisions.

II. COMPUTATIONAL METHOD

The geometry of the B^{3+}-H_2 system may be described by the internal Jacobi coordinates $\{R,r,\theta\}$ as defined in Fig. 1. The potentials have been determined for a large number of ion-H_2 distances in the 2–15 a.u range, as well as for different approaches θ from linear to perpendicular geometry, and various internuclear distances of the diatomic by means of multiconfiguration self-consistent-field calculations plus configuration interaction based on the configuration interaction by perturbation of a multiconfiguration wave function selected iteratively (CIPSIC) algorithm [11]. In order to provide the same description of the system in the different geometries, the calculations have been performed using the C_s symmetry group considering only the reflection on the (XY) plane containing the nuclei as symmetry operation, even in the linear approach. Relatively compact configuration-interaction spaces, of about 300–400 determinants for the zeroth-order diagonalization Hamiltonian, have been used in the calculation. Special care has been taken to construct sets of determinants providing the same level of accuracy over the whole potential-energy surface with a threshold $\eta=0.01$ for the perturbation contribution, providing a good description of the wave functions.

The basis of atomic functions used in the calculation is the $6s4p2d/4s2p$ basis of Gaussian functions previously optimized on the $B^{3+}(1s2s)+H$ collisional system [12]. It has been shown to provide a fair description of the $B^{2+}(1s2l2l')$ levels in the double capture process as well as a good agreement with the experimental data of Bashkin and Stoner [13] for single capture levels [12,14].

The radial coupling matrix elements between all pairs of

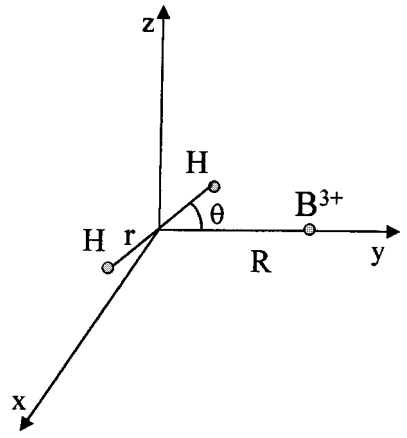

FIG. 1. Internal Jacobi coordinates (R,r,θ) used for $B^{3+}+H_2$.

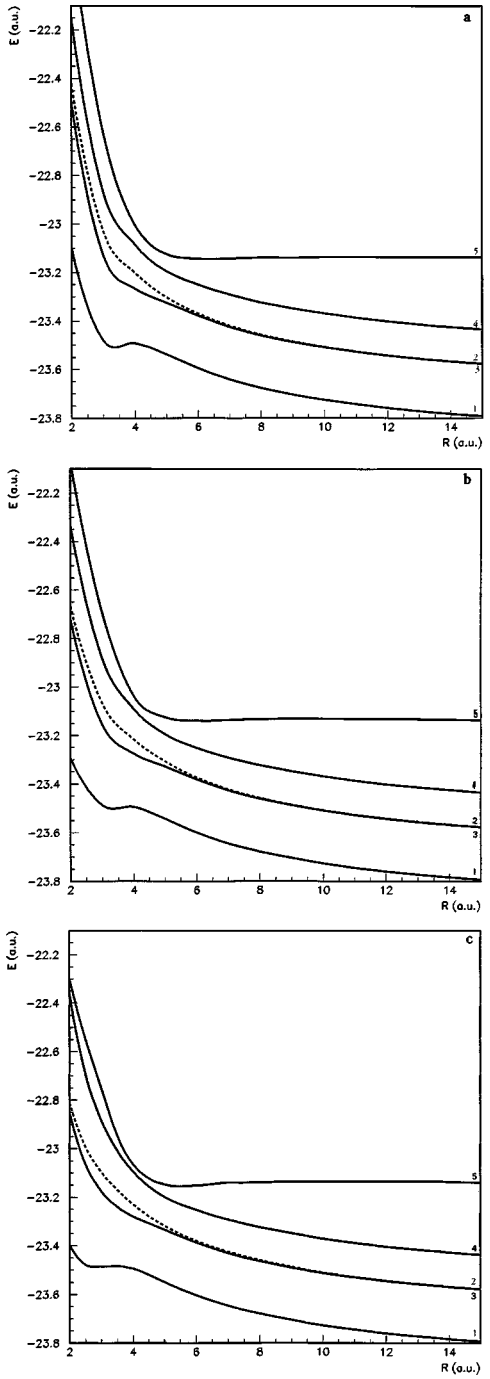

FIG. 2. Adiabatic potential-energy curves of the $^1A'$ and $^1A''$ states of BH_2^{3+} for $r=1.4$ a.u. (——, $^1A'$, -----, $^1A''$). (1) A' state dissociating to $\{B^{2+}(2s)^2S+H_2^+\}$, (2) A' state dissociating to $\{B^{2+}(2p)^2P+H_2^+\}$, (3) A'' state dissociating to $\{B^{2+}(2p)^2P+H_2^+\}$, (4) A' state dissociating to $\{B^+(2s^2)^1S+H^++H^+\}$, and (5) A' state dissociating to $\{B^{3+}(1s^2)^1S+H_2(^1\Sigma_g^+)\}$. (a) $\theta=0°$ (linear geometry), (b) $\theta=45°$, and (c) $\theta=90°$ (perpendicular geometry).

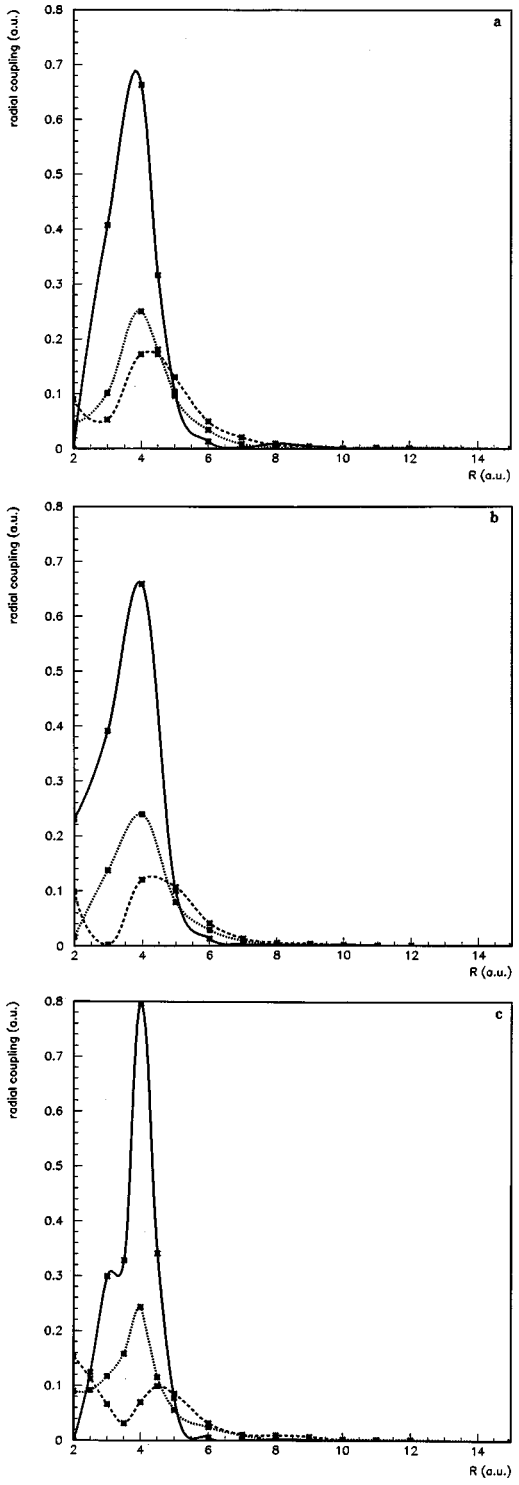

FIG. 3. Nonadiabatic radial coupling matrix elements between $^1A'$ states of BH_2^{3+} for $r=1.4$ a.u. (---------, g_{14}; ·····, g_{24}; ——, g_{45}). (a) $\theta=0°$ (linear geometry); (b) $\theta=45°$, and (c) $\theta=90°$ (perpendicular geometry).

states of the same symmetry have been calculated by means of the finite difference technique,

$$g_{KL}(R)=\langle\Psi_K|\partial/\partial R|\Psi_L\rangle=\lim_{\Delta\to 0} 1/\Delta\langle\Psi_K(R)|\Psi_L(R+\Delta)\rangle,$$

with the parameter $\Delta=0.0012$ a.u. as previously tested, and using the boron nucleus as origin of electronic coordinates. For reasons of numerical accuracy, we have performed a three-point numerical differentiation using calculations at $R+\Delta$ and $R-\Delta$ for a very large number of interatomic distances in the avoided crossing region, in particular for the sharp peaked coupling matrix elements.

For this approach of ion-molecule collisions, the rotational coupling matrix elements $\langle\Psi_K|iL_y|\Psi_L\rangle$ between mo-

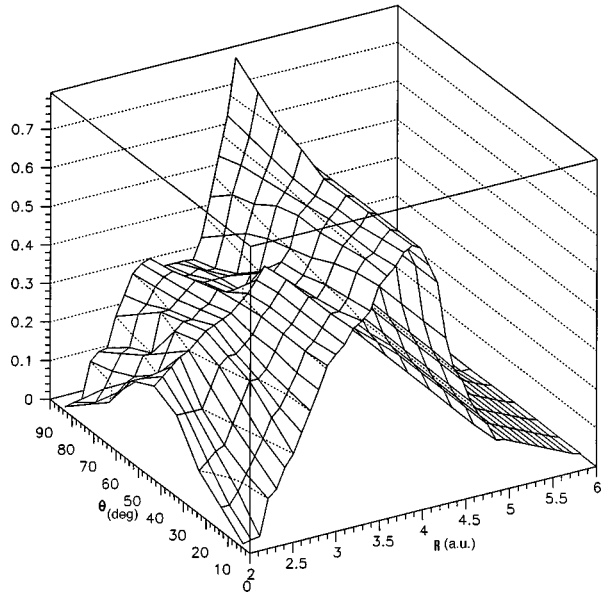

FIG. 4. Nonadiabatic radial coupling matrix element g_{45} between $^1A'$ states of BH_2^{3+} as a function of $(R,\theta)_{r=1.4\text{ a.u.}}$.

lecular states of different symmetries have not been taken into account in the calculation. Nevertheless, the quadrupole moment tensor between electronic wave functions has been determined, allowing the consideration of translation effects in the collision dynamics. In the approximation of the common translation factor [15], the radial coupling matrix elements between states Ψ_K and Ψ_L may indeed be transformed into

$$\left\langle \Psi_K \left| \frac{\partial}{\partial R} - (\epsilon_K - \epsilon_L) z^2/2R \right| \Psi_L \right\rangle,$$

where ϵ_K and ϵ_L are the electronic energies of states Ψ_K and Ψ_L, and z^2 the component of the quadrupole moment tensor. This expression, valid for any choice of electronic coordinates, has been used with the boron nucleus as origin of electronic coordinates.

III. MOLECULAR RESULTS

The presentation of the potential-energy surfaces and radial coupling matrix elements with respect to the R, r, and θ coordinates may be visualized successively as functions of $(R,\theta)_{r=Ct}$ and $(R,r)_{\theta=Ct}$ in the 2–15-a.u. range for R, and, respectively, in the 0°–90° range for θ and 1.2–1.6-a.u. range for r.

A. Anisotropy effect

The potential-energy curves as a function of the ion-H_2 distance, for different approaches of the B^{3+} ion, i.e., different values of the θ angle are displayed in Figs. 2(a)– 2(c) for a fixed value $r=1.4$ a.u. of the vibrational coordinate corresponding roughly to the equilibrium distance of the H_2 molecule. The corresponding radial coupling matrix elements are presented in Figs. 3(a)–3(c). As clearly observed, the main feature is an avoided crossing around $R=4.0$ a.u. between the double electron capture (DEC) channel correlated to

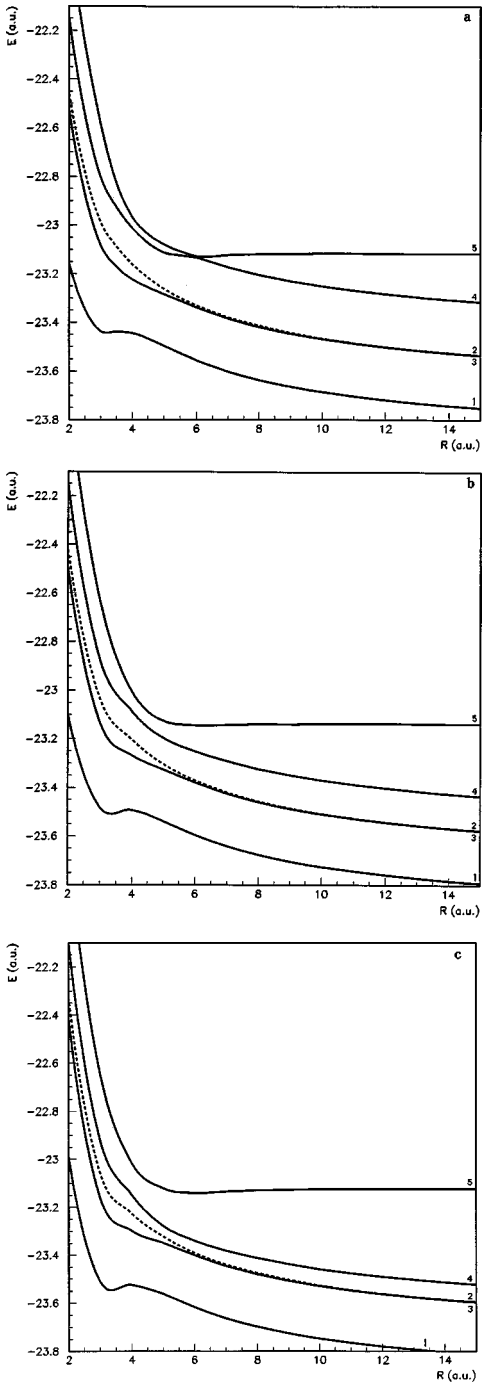

FIG. 5. Adiabatic potential-energy curves for the $^1A'$ and $^1A''$ states of BH_2^{3+} in the linear geometry ($\theta=0°$) (——, $^1A'$; -----, $^1A''$). (1) A' state dissociating to $\{B^{2+}(2s)^2S+H_2^+\}$, (2) A' state dissociating to $\{B^{2+}(2p)^2P+H_2^+\}$, (3) A'' state dissociating to $\{B^{2+}(2p)^2P+H_2^+\}$, (4) A' state dissociating to $\{B^+(2s^2)^1S+H^++H^+\}$, and (5) A' state dissociating to $\{B^{3+}(1s^2)^1S+H_2(^1\Sigma_g^+)\}$. (a) $r=1.2$ a.u., (b) $r=1.4$ a.u., and (c) $r=1.6$ a.u.

$B^+(2s^2)$ and the entry channel, corresponding to a sharp radial coupling matrix element g_{45}. The variation of this coupling matrix element as a function of θ and R is displayed in Fig. 4. It is nearly independent of the approach angle between $\theta=0°$ and $\theta=45°$, but is, however, more pronounced in the perpendicular geometry, in correspondence to the narrowing of the avoided crossing. This anisotropy is not correlated to a noticeable displacement in the position of the

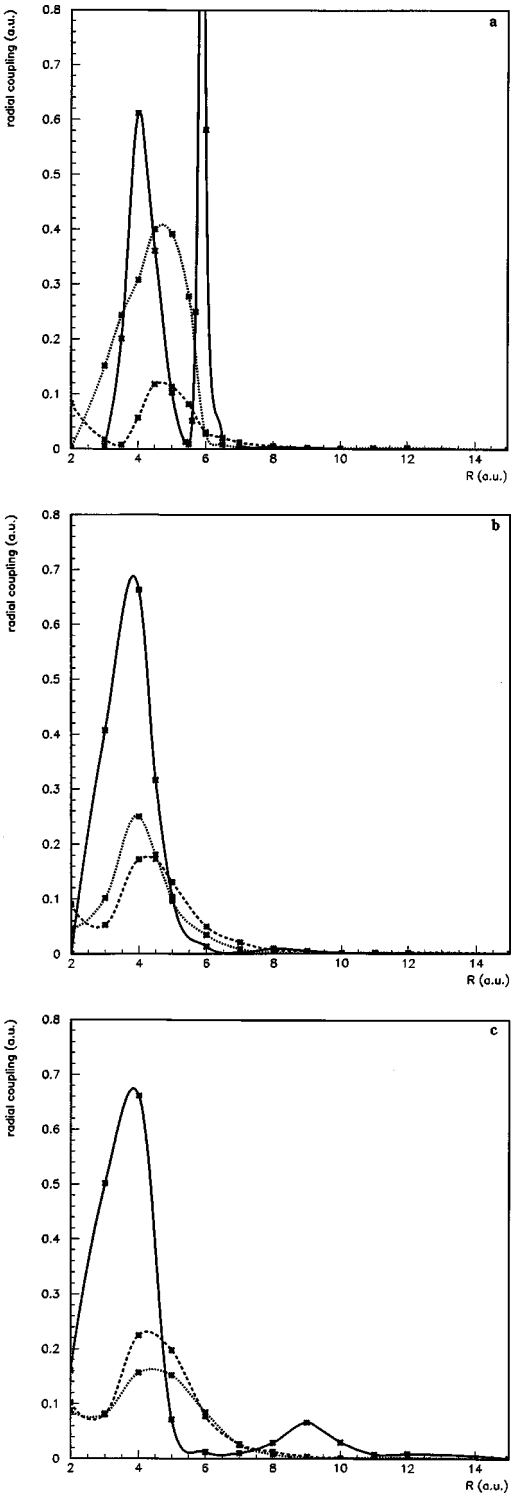

FIG. 6. Nonadiabatic radial coupling matrix element between $^1A'$ states of BH_2^{3+} in the linear geometry ($\theta=0°$) (---------, g_{14}; ·····, g_{24}; ——, g_{45}). (a) $r=1.2$ a.u., (b) $r=1.4$ a.u., and (c) $r=1.6$ a.u.

avoided crossing. A detailed picture of the radial coupling matrix elements shows besides a weak angular dependence for shorter distances R, in particular, a shouldering of the g_{45} matrix element in the perpendicular geometry. These remarks are almost independent of the internuclear distance r of the diatomic.

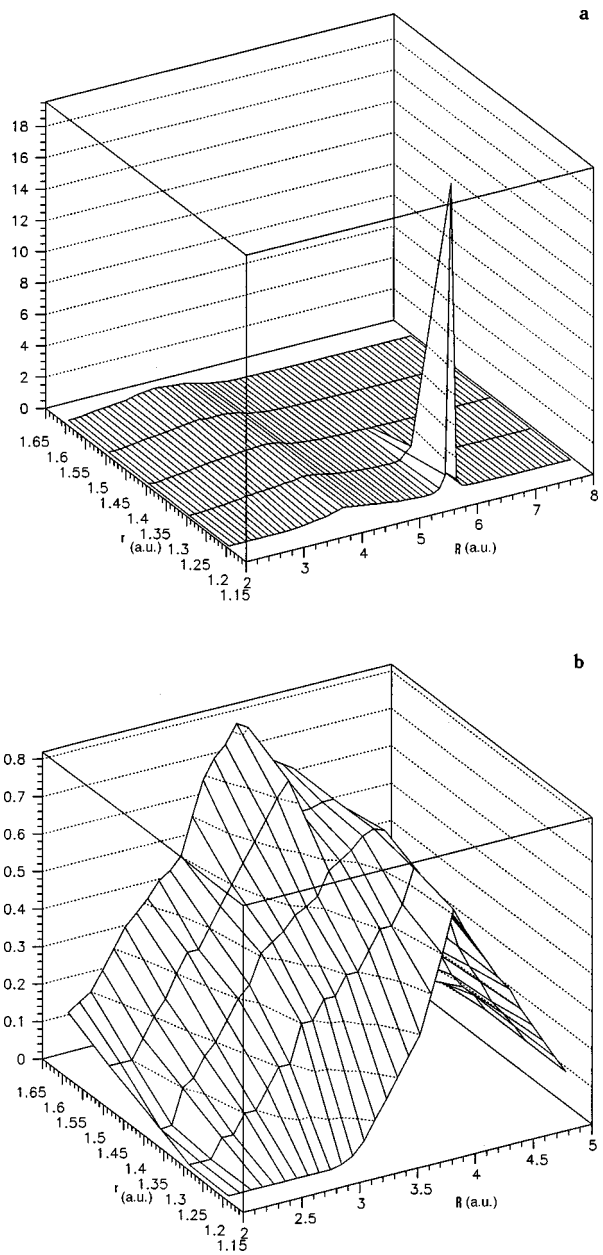

FIG. 7. Nonadiabatic radial coupling matrix element g_{45} between $^1A'$ states of BH_2^{3+} in the linear geometry as a function of $(R,r)_{\theta=0}$. (a) R (a.u.) $\in[2,8]$ and (b) R (a.u.) $\in[2,5]$.

B. Radial dependence

The variations of the $(R,r)_{\theta=Ct}$ potential-energy surfaces and radial coupling matrix elements are much more complicated. The results are presented in Figs. 5(a)–5(c) and Figs. 6(a)–6(c) for three values of the H-H distance in the linear geometry ($\theta=0°$). The main feature is the existence, for a relatively short $r=1.2$-a.u. distance, of a very pronounced avoided crossing between the entry channel and the $B^{2+}(2s^2)$ double capture level around $R=6.0$ a.u., in correspondence to a very sharp peak, up to 20.0 a.u. high, of the g_{45} radial coupling matrix element. The variation of the g_{45} radial coupling with respect to (R,r) for different ion-H_2 distance ranges, is visualized in Figs. 7(a) and 7(b). Such a coupling should lead first to a very diabatic crossing towards the double capture channel, followed by a significant avoided crossing around $R=4.0$ a.u. between this level and the entry

channel. For its part, the peak of the g_{45} radial coupling matrix element around $R=4.0$ a.u. is not markedly dependent on the interatomic distance of the diatomic, neither in position, nor in height. It is slightly narrowed with decreasing r values, in particular for the $r=1.2$ a.u. H-H distance, and its position is displaced towards short distances by less than 0.2 a.u. from $r=1.2-1.6$ a.u. This tendency has been already noticed by Errea *et al.* [3], but the behavior of $B^{3+}+H_2$ is relatively different from that observed in the case of $Be^{4+}+H_2$, where the position of the radial coupling was displaced by more than 2 a.u. and its amplitude divided by 5 from $r=1.2-1.7$ a.u. [3]. Apart of the peak around $R=6.0$ a.u. at $r=1.2$ a.u., the relative weak variations with the corresponding vibrational coordinate observed for the $B^{3+}+H_2$ collisional system for the g_{45} radial coupling around $R=4.0$ a.u. should validate the use of Franck-Condon-type approximations for collisional energies at least in the keV energy range.

IV. COLLISION DYNAMICS

The collision dynamics has been treated by a semiclassical approach using the EIKONXS program [16] based on an efficient propagation method in the 10–170-keV laboratory energy range. At the lower level of approximation, the molecular vibration can be ignored and the ion-molecule collision may be visualized as an ion bumping into an anisotropic atom. The total and partial capture cross sections, corresponding then to purely electronic transitions, may be determined by solving the impact-parameter equation as in the usual ion-atom approach, fixing the internuclear distance of H_2 at the $r_{eq}=1.4$ a.u. equilibrium nuclear separation. This approach has been shown to give reasonable total cross sections for energies greater than 100 eV/amu [5]. Assuming that the nuclear vibration and rotation periods are much longer than the collision time as in the sudden approximation method, an estimate of the vibrational motion of the diatomic molecule, neglecting the rotational modes of H_2, may be obtained by introducing Franck-Condon factors in the framework of the centroïd approximation,

$$\sigma_{0\nu}^{\mathrm{FC}}(v)=\sigma^{el}(r_{\mathrm{eq}},v)F_{0\nu}, \tag{1}$$

where $F_{0\nu}$ is the Franck-Condon factor between the H_2 and H_2^+ vibrational wave functions,

$$F_{0\nu}=\langle \chi_0^{H_2}(r_{\mathrm{eq}})|\chi_\nu^{H_2^+}(r_{\mathrm{eq}})\rangle^2. \tag{2}$$

This approximation is very crude and supposes that the vibrational distribution depends only on Franck-Condon factors, neglecting possible asymptotic energy defects [5]. It has been widely discussed by Errea *et al.* [17] on the $Be^{4+}+H_2$ collisional system and, while not satisfactory at low energies, it has been shown to provide nevertheless a reasonable accuracy for impact energies greater than 500 eV/amu, in the energy range we are dealing with in this paper. Furthermore, the relatively weak variations with r observed for the g_{45} radial coupling matrix element around $R=4.0$ a.u. compared to that exhibited in the $Be^{4+}+H_2$ system may give confidence in the use of such an approximation for an approach of this ion-H_2 collisional process.

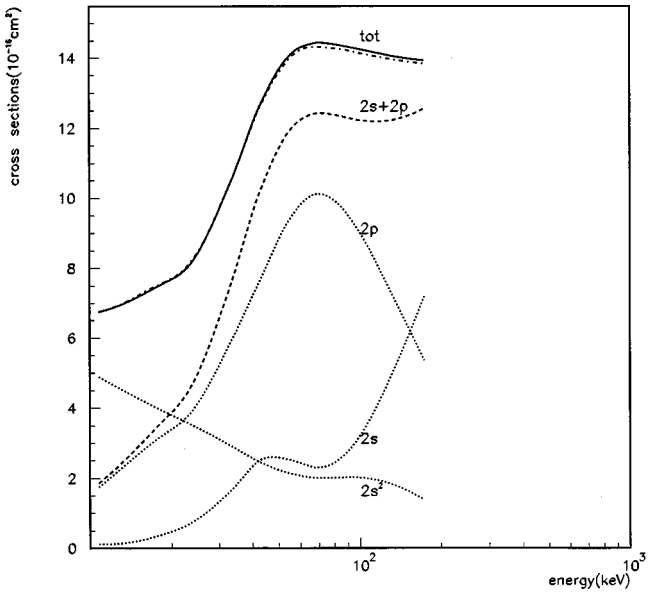

FIG. 8. Total and partial cross sections for the $\{B^{3+}+H_2\}$ system in the linear geometry, with respect to laboratory energies (——, σ_{tot} with translation; -·-·-, σ_{tot} without translation; ------, σ_{2s+2p} with translation; and ·····, σ_{2s}, σ_{2p}, and σ_{2s^2} with translation).

The calculation has been performed in the linear geometry and translation effects have been investigated. The results presented in Fig. 8 show clearly that translation effects are negligible for this system all over the energy range of interest. The partial cross sections on the $2s$, $2p$, and $2s^2$ levels are also presented exhibiting the important contribution of single electron capture (SEC) in the total process; the double capture is yet not negligible but decreases with increasing collisional energy. The total, single, and double electron-capture cross sections averaged over the different approach angles θ for taking account of the anisotropy dependence of the collisional system are given in Table I and drawn in Fig. 9 with comparison to experimental data. The shape of the cross sections is quite similar to that observed in the linear geometry, in accordance with the weak θ dependence exhibited by the molecular calculations. The experimental data are relatively sparse at lower energies, but remain coherent and may be visualized as proposed by Janev, Winter,

TABLE I. Orientation-averaged cross sections for $B^{3+}+H_2$ (in $10^{-16}\,\mathrm{cm}^2$).

v (a.u.)	E_{lab} (keV)	σ_{2s}	σ_{2p}	σ_{SEC}	σ_{DEC}	σ_{tot}
0.2	10.80	0.14	1.55	1.70	4.60	6.30
0.25	16.88	0.36	2.94	3.30	3.83	7.13
0.3	24.30	0.86	4.10	4.96	3.16	8.12
0.35	33.08	1.68	5.79	7.47	2.39	9.86
0.4	43.20	2.56	7.50	10.06	1.80	11.86
0.45	54.68	2.67	9.23	11.90	1.50	13.40
0.50	67.51	2.53	10.25	12.79	1.40	14.20
0.55	81.60	2.72	10.32	13.03	1.42	14.45
0.60	97.21	3.32	9.70	13.01	1.43	14.44
0.70	132.32	5.31	7.611	12.92	1.25	15.17
0.80	172.82	7.59	5.42	13.02	0.94	13.96

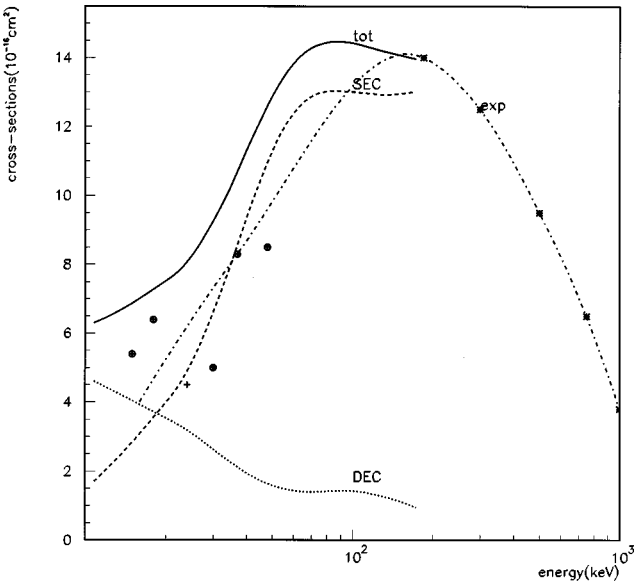

FIG. 9. Orientation-averaged total and single electron-capture cross sections for the $\{B^{3+}+H_2\}$ system with respect to laboratory energies (——, σ_{tot}; ---------, σ_{SEC}; ·····, σ_{DEC}; -·-·-·-·-, σ_{exp} [18]) +, Gardner *et al.* [6]; ⊕, Crandall, Phaneuf, and Meyer [7]; and ∗, Goffe, Shah, and Gilbody [8].

and Fritsch [18]. Our results reproduce reasonably well their tendency with an increase of the cross sections up to about 100 keV and a decrease for higher collisional energies, as in Goffe's experiments [8].

The vibrational behavior of the H_2 molecule during the collisional process has been evaluated by using Eq. (1). The vibrational energy levels and Franck-Condon factors have been calculated in the anharmonic approximation by means of the Hutson's method [19], valid for vibrational levels even near dissociation, taking for H_2 the energy curve of Kolos and Wolniewicz [20], and for H_2^+ the potentials determined by means of an elliptical orbital method using the ODKIL code [21]. The partial cross sections of single electron capture in the $B^{3+}(^1S)+H_2(\nu=0)$ collision, $\sigma_{0\nu}^{FC}(v)$, are displayed in Table II. They show a maximum of the capture on the $\nu=2$ vibrational level of H_2^+. Unfortunately, no experimental data was available for comparison.

TABLE II. Partial cross sections for the $B^{3+}+H_2(\nu=0)\rightarrow B^{2+}+H_2^+(\nu)$ charge-transfer process (in $10^{-16}\,cm^2$) for different collision velocities v (in a.u.).

ν	$v=0.2$	$v=0.25$	$v=0.3$
0	0.154	0.300	0.450
1	0.272	0.529	0.793
2	0.296	0.575	0.862
3	0.259	0.505	0.756
4	0.203	0.395	0.592
5	0.149	0.290	0.435
6	0.106	0.206	0.308
7	0.074	0.143	0.215
8	0.051	0.099	0.149
9	0.035	0.069	0.103
10	0.024	0.048	0.072
11	0.017	0.033	0.050
12	0.012	0.023	0.035

V. CONCLUDING REMARKS

This work provides accurate *ab initio* potential-energy surfaces and radial coupling matrix elements for the $B^{3+}+H_2$ collisional system. The anisotropy dependence has been shown to be relatively weak for this ion-molecule reaction. The collision dynamics exhibits an important contribution of single electron capture, even though double electron capture should be taken into account. Some further experimental data should be welcome for a more precise comparison, in particular, concerning the description of the vibrational motion of the diatomic molecule.

[1] P. C. Stancil, P. S. Krstić, and D. R. Schultz, in *Atomic Processes in Plasmas*, edited by E. Obs and M. S. Pindzola (AIP, New York, 1998), p. 185.

[2] L. F. Errea, J. D. Gorfinkiel, C. Harel, H. Jouin, A. Macías, L. Méndez, B. Pons, and A. Riera, Phys. Scr. **T62**, 33 (1996).

[3] L. F. Errea, J. D. Gorfinkiel, E. S. Kryachko, A. Macías, L. Méndez, and A. Riera, J. Chem. Phys. **106**, 172 (1997).

[4] L. F. Errea, J. D. Gorfinkiel, A. Macías, L. Méndez, and A. Riera, in *Proceedings of the IX International Conference on the Physics of Highly Charged Ions, Bensheim, 1998*, edited by P. H. Mokler (The Royal Swedish Academy of Sciences, Stockholm, in press).

[5] P. C. Stancil, B. Zygelman, and K. Kirby, in *Photonic, Electronic, and Atomic Collisions*, edited by F. Aumayr and H. P. Winter (World Scientific, Singapore, 1998), p. 537.

[6] L. D. Gardner, J. E. Bayfield, P. M. Koch, I. A. Sellin, D. J. Pegg, R. S. Peterson, M. L. Mallory, and D. H. Crandall, Phys. Rev. A **20**, 766 (1979).

[7] D. H. Crandall, R. A. Phaneuf, and F. W. Meyer, Phys. Rev. A **19**, 504 (1979); D. H. Crandall, *ibid.* **16**, 958 (1977).

[8] T. V. Goffe, M. B. Shah, and H. B. Gilbody, J. Phys. B **12**, 3763 (1979).

[9] F. Fraija, M. Druetta, D. Hitz, and M. C. Bacchus-Montabonel, in *Proceedings of the VII International Conference on the Physics of Highly Charged Ions, Vienna, 1994*, edited by F. Aumayr, G. Betz, and H. P. Winter (North-Holland, Amsterdam, 1995); F. Fraija, Doctorate thesis, University of Lyon, Lyon, France, 1994 (unpublished).

[10] R. K. Janev, Phys. Scr. **T62**, 5 (1996).

[11] B. Huron, J. P. Malrieu, and P. Rancurel, J. Chem. Phys. **58**, 5745 (1973).

[12] M. C. Bacchus-Montabonel and F. Fraija, Phys. Rev. A **49**, 5108 (1994).

[13] S. Bashkin and J. O. Stoner, *Atomic Energy Levels and Grotrian Diagrams* (North-Holland, Amsterdam, 1975).

[14] M. C. Bacchus-Montabonel, Phys. Rev. A **53**, 3667 (1996).

[15] L. F. Errea, L. Méndez, and A. Riera, J. Phys. B **15**, 101 (1982).
[16] R. J. Allan, C. Courbin, P. Salas, and P. Wahnon, J. Phys. B **23**, L461 (1990).
[17] L. F. Errea, J. D. Gorfinkiel, A. Macías, L. Méndez, and A. Riera, J. Phys. B **30**, 3855 (1997).
[18] R. K. Janev, H. P. Winter, and W. Fritsch, in *Atomic and Molecular Processes in Fusion Edge Plasmas*, edited by R. K. Janev (Plenum, New York, 1995), p. 341.
[19] J. M. Hutson, J. Phys. B **14**, 851 (1981).
[20] W. Kolos and L. Wolniewicz, J. Chem. Phys. **49**, 404 (1968).
[21] M. Frécon (private communication).